Neuron-selective toxicity of tau peptide in a cell culture model of neurodegenerative tauopathy: Essential role for aggregation in neurotoxicity

ARTICLE *in* JOURNAL OF NEUROSCIENCE RESEARCH · NOVEMBER 2010

Impact Factor: 2.59 · DOI: 10.1002/jnr.22485 · Source: PubMed

Journal of Neuroscience Research

Journal of Neuroscience Research 88:3399–3413 (2010)

Neuron-Selective Toxicity of Tau Peptide in a Cell Culture Model of Neurodegenerative Tauopathy: Essential Role for Aggregation in Neurotoxicity

**Kelly Zhao,[1] Giulia Ippolito,[1] Lulu Wang,[1] Valerie Price,[1] Mi Hwa Kim,[2] Gavin Cornwell,[2] Stephanie Fulenchek,[2] Gail A. Breen,[1] Warren J. Goux,[2] and Santosh R. D'Mello[1]*

[1]Department of Molecular and Cell Biology, University of Texas at Dallas, Richardson, Texas
[2]Department of Chemistry, University of Texas at Dallas, Richardson, Texas

Intracellular aggregation of tau is a pathological hallmark in Alzheimer's disease and other tauopathies. The mechanisms underlying tau aggregation and the role that these aggregates play in neuronal death have remained controversial. To study these issues, we established a cell culture model of tauopathy using a hexameric peptide with the sequence ^{306}VQIVYK^{311} located within the third microtubule-binding repeat of tau, rendered cell-permeable by a tag of nine arginine residues (R_9). This peptide (VQIVYK-R_9), designated as T-peptide, self-assembles in vitro into paired helical filament-like aggregates. Primary neuronal cells treated with T-peptide die within 24 hr. Neurodegeneration correlates with the ability of the peptide to aggregate. Two peptides with mutations in the hexameric core, K-peptide (VQIVKK) and VV-peptide (VQVVVK), that are incapable of aggregating are not toxic, whereas two other mutant peptides, V-peptide (VQVVYK) and F-peptide (VQIVFK), which aggregate, are also neurotoxic. Two other peptides that aggregate in vitro, but are not derived from tau, are not neurotoxic suggesting sequence dependence. Although localizing to the nucleus, T-peptide induces aggregation of cellular proteins in the cytoplasm. These aggregates are not caused by disruption of endogenous tau localization, although endogenous tau is reduced in neurons exposed to T-peptide. Interestingly, nonneuronal cells are less sensitive to T-peptide toxicity, recapitulating in part the selective loss of neurons in tauopathies. Moreover, T-peptide treatment leads to mitochondrial dysfunction, a common feature of neurodegenerative disorders. The model system described here represents a convenient paradigm for studying the mechanisms underlying tau aggregation and neurotoxicity and for identifying compounds that can prevent these effects.

Key words: Alzheimer's disease; tau proteins; tauopathies; neurodegenerative diseases; neuronal cell death

A major pathological hallmark of Alzheimer's disease (AD) and other tauopathies is the formation of neurofibrillary tangles (NFTs) within neurons of the brain (Feany and Dickson, 1996; Ballatore et al., 2007; Honson and Kuret, 2008). NFTs are composed of insoluble twisted filaments, known as paired helical filaments (PHFs), made up of aggregated tau, a microtubule-associated protein. Because the appearance of NFTs correlates with neuronal death and loss of cognitive function in AD, it is generally believed that aggregated tau has a toxic effect on neurons.

Tau is a protein expressed predominantly in neurons, where it functions to promote tubulin polymerization and microtubule stability. Under normal circumstances, it is a highly soluble protein, showing little tendency to aggregate. Its aggregation into filaments in neurodegenerative pathologies is accompanied by abnormal posttranslational modifications, the best studied of which is hyperphosphorylation (for review see Castellani et al., 2008). Another modification gaining considerable attention is cleavage of tau by proteases, including caspases and calpains. Indeed, tau cleavage has been observed in AD as well as in experimental models of neurodegeneration (Canu et al., 1998; Gamblin et al., 2003; Corsetti et al., 2008). Although there is agreement that tau assembles into PHFs, is phosphorylated, and can be proteolyzed, the relationship among these different modifications and their significance to neurodegeneration remain unclear and are a topic of much disagreement. For example, although it is generally believed that hyper-

K. Zhao and G. Ippolito contributed equally to this work.

Contract grant sponsor: National Institutes of Health; Contract grant number: NS040408 (to S.R.D.); Contract grant number: NS047201 (to S.R.D.); Contract grant sponsor: University of Texas at Dallas (to W.G., G.A.B.).

*Correspondence to: Santosh D'Mello, Department of Molecular and Cell Biology, University of Texas at Dallas, 800 W. Campbell Road, Richardson, TX 75080. E-mail: dmello@utdallas.edu

Received 18 May 2010; Revised 17 June 2010; Accepted 18 June 2010

Published online 29 September 2010 in Wiley Online Library (wileyonlinelibrary.com). DOI: 10.1002/jnr.22485

phosphorylation of tau leads to its aggregation, emerging evidence suggests that tau phosphorylation actually inhibits its aggregation (Schneider et al., 1999; Wang et al., 2007). Other studies have suggested that aggregation of tau into PHFs is not directly neurotoxic (Andorfer et al., 2005) or that formation of tau filaments protects against the neurotoxic effects of hyperphosphorylated tau (Alonso Adel et al., 2006). More recently, smaller prefibrillar tau aggregates or soluble tau monomers have been suggested to be the toxic species (Santacruz et al., 2005; Berger et al., 2007; Ding and Johnson, 2008).

Our study is based on three sets of recent observations. First, work performed both in vitro and in cultured cells has shown that proteolytic fragments of tau containing the microtubule-binding repeat regions aggregate robustly, forming AD-like PHFs (von Bergen et al., 2000, 2001). Second, such aggregated fragments of tau are able to nucleate the aggregation of full-length tau both in cultured cells and in transgenic mice (Mocanu et al., 2008b; Wang et al., 2007; Frost et al., 2009). Third, a six-amino-acid region, ^{306}VQIVYK^{311}, located within the third microtubule-binding repeat of tau has been identified as the smallest sequence of tau capable of assembly into pathological PHFs (von Bergen et al., 2000). We and others have previously shown that this hexapeptide has a very high propensity for self-aggregation (von Bergen et al., 2000; Goux et al., 2004; Rojas Quijano et al., 2006). Deletion of this six-amino-acid sequence from full-length tau dramatically reduces the ability of tau to aggregate in transfected cells (Sahara et al., 2007).

Because the hexameric motif can self-aggregate and promote assembly of full-length tau into PHF-like filaments, we tested the hypothesis that intracellular delivery of this hexapeptide would be sufficient to induce neurotoxicity. We report that a cell-permeable peptide composed of the VQIVYK sequence (designated as T-peptide) is, in fact, a potent inducer of neuronal death. Its ability to kill nonneuronal cells is substantially lower, recapitulating the selective loss of neurons in AD and other neurodegenerative tauopathies. Furthermore, treatment of neuronal cells with T-peptide results in mitochondrial dysfunction, another hallmark of neurodegenerative disorders.

MATERIALS AND METHODS

Unless mentioned otherwise, all chemicals were purchased from Sigma-Aldrich (St. Louis, MO). Tissue culture reagents including cell culture medium, fetal calf serum (FCS), poly-L-lysine, L-glutamine, penicillin-streptomycin, and gentamycin were from Invitrogen (Carlsbad, CA). LC3 and total tau antibody was also from Sigma-Aldrich. Tau-pSer404 and Tau-pSer262 antibodies were from Santa Cruz Biotechnology (Santa Cruz, CA). Fluorescence-conjugated secondary antibodies were from Jackson Immunoresearch (West Grove, PA). The tau-YFP plasmid was kindly provided by Dr. Marc Diamond (Washington University School of Medicine).

Peptides

N-acetyl peptide amides Ac-vqivyk-R_9-NH_2 (T-peptide; lower case amino acid codes denote D-amino acids), Ac-vqivyk-NH_2 (core peptide), Ac-vqvvyk-R_9-NH_2 (V-peptide), Ac-vqvvvk-R_9-NH_2 (VV-peptide), Ac-vqivkk-R_9-NH_2 (K-peptide), Ac-VQIVYK-R_9-NH_2 [T(L)-peptide], Ac-STVIIE-R_9-NH_2 (ST-peptide), Ac-SQIVYA-R_9-NH_2 (SQ-peptide), and Ac-vqivfk-R_9-NH_2 (F-peptide) were prepared by solid-phase peptide synthetic methods according to previously published procedures and purified by reverse-phase HPLC using a water-acetonitrile gradient (Goux et al., 2004; Rojas Quijano et al., 2006). An FITC-labeled version of T-peptide (FITC-T-peptide) was prepared from a resin-bound T-peptide having two N-terminal amino hexanoic "linker residues" onto which 5′(6)-carboxyfluorescein was coupled using standard solid-phase methodology. Peptide purity was checked using MALDI-TOF MS. Stock solutions of the peptides were prepared (~1 mg/ml) in deionized water. Final concentrations determined by weight, assuming the TFA salt of the purified peptide, agreed within 5% of concentrations determined using the reported molar extinction coefficients for tyrosine [ε_{276} of 1,390 $M^{-1}cm^{-1}$ (Ventura et al., 2004)] or for the peptide bond [ε_{192} of 7110 $M^{-1}cm^{-1}$ (Vauthey et al., 2002)].

Transmission Electron Microscopy

Filtered stock peptide solutions were diluted to 100 μM in 5 mM MOPS containing 0.1% NaN_3, 0.15 M NaCl, pH 7.2 (buffer A), and were incubated at room temperature overnight. Samples were loaded onto carbon-coated Formvar copper grids (200 mesh) and stained with 2% wt/wt uranyl acetate. A JEOL 1200EX scope interfaced to a digital camera was used to visualize samples.

Kinetic Analysis

Polymerization kinetics were measured by monitoring the increase in thioflavin-S (ThS) fluorescence at 490 nm (440 nm excitation). Slit widths were 15 and 20 nm, respectively, for excitation and emission. All measurements were carried out at 21°C with a Perkin Elmer LS50B spectrofluorimeter using a 75-μl quartz cell. Data points were collected at 6-sec intervals over the course of the experiment (up to 180 min). To initiate polymerization, a freshly prepared solution of the peptide in water was filtered using Amicon Ultra Centrifugal Filters (100K MW cutoff) and diluted to 10 μM in 200 μl buffer A containing 33 μM heparin (Sigma-Aldrich; 3,000 MW) and 100 μM ThS. Kinetic data, corrected for the blank, were fit using a nonlinear least squares algorithm to a Gompertz-like growth curve (Necula and Kuret, 2004). Those kinetic curves having no lag times were fit to Equation 1:

$$y = e^{-k't}Ae^{-e^{\left(\frac{(t-t_i)}{b}\right)}}, \quad (1)$$

where y is defined as the fluorescence signal at time t, t_i corresponds to the inflection point of the curve or the time of maximum growth rate, A is the maximum fluorescence observed for a given sample, and b = 1/k, where k is the rate constant of aggregation, in units of sec^{-1}. The pregrowth

curve exponential, $e^{(-k't)}$, was inserted to take into account the slow decrease in fluorescent intensity resulting from ThS bleaching, quenching, and gravitational precipitation of the amyloid-ThS complex. The kinetic curve for ST-peptide showed a slow aggregation followed by a significant lag time and a second rapid aggregation and was fit to Equation 2:

$$y = Ae^{-e^{\left(\frac{(t-t')}{b}\right)}} + A'e^{-e^{\left(\frac{(t-t'')}{b'}\right)}}, \quad (2)$$

where $k' = 1/b'$, the lag time is calculated as t''-b', and other terms are as defined as for Equation 1. Standard errors in fitted parameters were estimated assuming a 10% error in the sum of the squares.

Culture and Treatment of Neurons

Cerebellar granule neurons were cultured from 7–8-day-old rats as previously described (D'Mello et al., 1993). The neurons were plated in 24-well batches with poly-L-lysine-coated glass coverslips at a density of ~1 million cells/well in basal Eagle's medium with Earle's salts (BME) supplemented with 10% FCS, 25 mM KCl, 2 mM glutamine, and 100 mg/ml gentamicin. To prevent mitosis of glial cells, cytosine arabinofuranoside (10 μM) was added to cultures 16–20 hr after plating. Neuronal cultures were treated with peptides 6–7 days after plating. For treatment, the cultures were switched to serum-free medium containing 25 mM KCl (referred to as high-potassium or HK medium). Although serum is required for proper maturation, after 5 days in culture, the neurons survive normally in the absence of serum provided that depolarizing levels of KCl are added (D'Mello et al., 1993).

Cultures of Kidney Fibroblasts and Treatment With Peptides

Kidneys were taken from 7–8-day-old rats and placed in Dulbecco's modified Eagle's medium (DMEM). They were then diced and trypsinized for 8–12 min. Trypsin was inactivated with trypsin inhibitor and centrifuged at 500*g* for 1 min. Pellets were resuspended in DMEM and broken up with a pasteur pipette 25 times, then centrifuged at 1,000*g* for 1 min. Again the pellet was resuspend in DMEM, broken up with Pasteur pipette, and centrifuged at 1,000*g*. After resuspending pellets in DMEM, the cells were centrifuged again at 500*g* for 10 min. The cell pellet was then dissociated and plated in DMEM supplemented with 10% FCS, 50 U/ml penicillin, and 50 μg/ml streptomycin in 24-well dishes. Treatment with peptides was done at 40–50% confluence for Live/Dead assays and 80–90% confluence for MTT assays.

HT-22 and HEK293 Cell Culture

HT-22 cells were maintained in DMEM supplemented with 10% FCS, 50 U/ml penicillin and 50 μg/ml streptomycin. HEK293 cells were maintained in DMEM supplemented with 10% FCS, 50 U/ml penicillin, and 50 μg/ml streptomycin. Both cell lines were treated with peptide at 70–80% confluence in serum-free media.

Cell Viability Quantification

Cell viability was quantified using the Live/Dead assay with a commercially available kit (Invitrogen). This is a two-color fluorescence assay utilizing two cell-permeable compounds, calcein acetoxymethyl (calcein AM) and ethidium homodimer-1 (EthD-1). Live cells have intracellular esterases that convert nonfluorescent calcein AM to the intensely green fluorescent calcein, which is retained within the cytoplasm of cells. Because dead cells have damaged membranes, EthD-1 enters and is fluorescent when bound to nucleic acids. EthD-1 stains the nuclei of damaged or dead cells. As recommended by the manufacturer, cells plated in wells with coverslips were incubated in Live/Dead reagent (1 μM calcein AM and 4 μM EthD-1) for 30 min and then mounted on slides. Cell viability was also analyzed using the MTT [3-(4,5-dimethylthiazol-2-yl)-2,5-diphenyltetrazolium bromide] assay based on the evaluation of mitochondrial function. MTT assays were performed as previously described (Koulich et al., 2001). Briefly, MTT (5 mg/ml in culture medium) was added to the culture medium, and the cells were incubated at 37°C for 1 hr. The assay was stopped by adding lysis buffer [20% sodium dodecyl sulfate (SDS) in 50% N,N-dimethylformamide, pH 4.7]. Absorbance was measured spectrophotometrically at 570 nm after an overnight incubation at room temperature.

Western Blot Analysis

Cells were washed once with ice-cold phosphate-buffered saline (PBS) and lysed using lysis buffer (1% Triton, 20 mM Tris-HCl, pH 7.5, 150 mM NaCl, 1 mM sodium EDTA, 1 mM EGTA, 2.5 mM sodium pyrophosphate, 1 mM β-glycerophosphate, 1 mM Na_3VO_4,1 μg/ml leupeptin, and one protease inhibitor tablet). Protein concentration was measured with Bradford assay reagent (Bio-Rad, Hercules, CA). Protein concentration was normalized to 50–75 μg, and 6× SDS was added to each sample. Samples were run on 15% denaturing gels and transferred to PVDF membrane and then blocked for 1 hr and incubated with primary antibody. The dilutions used were LC3 antibody,1:1,000 dilution; tau, 1:1,000 dilution; tau-pSer404 and tau-pSer262, 1:1,000 dilution. After washes, the membrane was incubated with horseradish peroxidase-conjugated secondary antibody. After the incubation, membranes were washed and developed with Enhanced Chemiluminescence reagent (Amersham Biosciences, Arlington Heights, IL).

Immuocytochemistry

The cells were fixed with 4% paraformaldehyde in PBS and washed three times using 0.1 M PBS containing 0.5% Triton before blocking with 0.1 M PBS containing 1% BSA and 5% goat serum for 15 min. Immunostaining was performed by incubation with tau antibody (1:200 dilution) overnight at 4°C. The secondary antibody was incubated for 45 min at 25°C. Cell nuclei were stained with DAPI for 15 min at 25°C. Staining was visualized by fluorescence microscopy.

Transfection of Neurons and HT-22 Cells

Transfection of neurons and HT-22 cells was performed as previously described (Chen et al., 2008; Majdzadeh et al.,

2008). Briefly, cerebellar granule neurons were transfected on day 5 after plating using the cacium phosphate method. HT-22 cells were transfected using Lipofectamine 2000 (Invitrogen). The cultures were treated with peptides the day after transfection and effects were evaluated 24 hr later.

Staining of Tau Aggregates

Aggregates were stained with ThS and counterstained with propidium iodide (PI) for dead cells and 4′,6-diamidino-2-phenylindole (DAPI) for the nucleus of all cells. One to three hours after treatment with peptide, cells were incubated in media containing 20 μg/ml PI for 10 min, washed three times with media, incubated in cold 4% paraformaldehyde for 10 min, washed with PBS, incubated in 0.1% Triton X-100 for 5 min, incubated in DAPI for 10 min, and washed with PBS. Improved ThS staining technique was employed (Sun et al., 2002). Briefly, the fixed cells were incubated in 0.01% ThS, washed three times with 70% ethanol for 5 min each, washed with water, incubated in 0.25% $KMnO_4$ for 4 min, washed with water, incubated in 1% $NaBH_4$ for 4 min, and then again washed with water. Cells were mounted on slides using Fluoromount-G mounting media (Southern Biotech, Birmingham, AL).

Mitochondrial Membrane Potential Assay

The mitochondrial membrane potential of cells was determined using the cationic dye JC-1 (5,5′,6,6′-tetra chloro-1,1′,3,3′-tetraethylbenzimidazolylcarbocyanineiodide). JC-1 accumulates in mitochondria in a potential-dependent manner (Reers et al., 1991). When JC-1 selectively enters mitochondria, it changes fluorescence from a monomeric green form to red fluorescent J-aggregates (Reers et al., 1991). A decrease in the red to green fluorescence intensity ratio indicates depolarization of mitochondria. Cells were plated into black 96-well plates (Corning), grown at 37°C, and then peptides were added to the cells in DMEM without serum for 24 hr. The medium was removed, 5 μM of JC-1 (Biotium) in DMEM without serum was added, and plates were incubated for 2 hr at 37°C. Cells were washed three times with PBS, and then 100 μl of PBS was added to each well. Fluorescence was measured using a Gemini fluorescent microplate reader (Molecular Devices, Sunnyvale, CA) with an excitation wavelength of 485 nm and an emission wavelength of 538 nm to detect green fluorescence and excitation/emission wavelengths of 544/590 nm to detect red fluorescence. As a positive control, valinomycin (100 μM) was used to depolarize the mitochondrial membrane potential.

Analysis of Viability Data

Unless indicated otherwise, data are given as mean ± standard deviation. For statistical significance, data were evaluated at a 0.05 level of significance with the Bonferroni ANOVA.

RESULTS

Generation and Aggregation Analysis of Tau Peptides

Previous studies have shown that tau polymerization involves the formation of a β-sheet structure arising from short hexapeptide motifs in the second and third repeat of tau, specifically ^{275}VQIINK^{280} in microtubule-binding repeat R2 and ^{306}VQIVYK^{311} in repeat R3 (von Bergen et al., 2000; Barghorn and Mandelkow, 2002). We and others have previously shown that the R3 hexapeptide Ac-^{306}VQIVYK^{311}-NH_2 could, by itself, self-nucleate and form fibrils in vitro (Goux et al., 2004; Rojas Quijano et al., 2006; von Bergen et al., 2006). To render this hexapeptide cell-permeable, we attached an HIV Tat-like motif composed of nine arginine residues (R_9) to the C-terminal. Arginine-rich peptides translocate the plasma membrane efficiently and are used for intracellular delivery of macromolecules and chemicals (Futaki et al., 2001; Futaki, 2002; Suzuki et al., 2002; Allen et al., 2004). The hexameric core was synthesized with D-amino acids, and the R_9 tag was composed of L-arginine. The rationale for synthesizing a D-core was twofold; first, it would be more stable against proteolytic degradation and, second, the D-version would not bind to specific protein targets within the cell thus allowing a better evaluation of the effect of aggregation itself on cell survival. The vqivyk-R_9 peptide was designated as T-peptide. Neurotoxicity studies were also carried out on the T-peptide lacking the R_9 tag, vqivyk, which we designate as the core-peptide. Mutants of the T-peptide, vqvvyk-R_9 (V-peptide), vqvvvk-R_9 (VV-peptide), vqivkk-R_9 (K-peptide), and vqivfk-R_9 (F-peptide), were also studied to determine whether toxicity was a function of primary structure and the ability of these peptides to self-associate into aggregates. Table I summarizes the structures and abbreviations for the peptides used in this study.

Self-Association of Peptides In Vitro

We measured the self-association behavior of our peptides in vitro in the presence of the polyanion heparin, by following the enhancement of fluorescence arising from the binding of ThS to amyloid. We have previously shown that the L-amino-acid version of the core-peptide, Ac-vqivyk-NH_2 (previously referred to as AcPHF6), readily polymerizes into amyloid fibrils above a critical concentration of about 2 μM (Goux et al., 2004; Rojas Quijano et al., 2006). The polymerization kinetics (shown in Fig. 1) suggest that T-peptide, V-peptide, and F-peptide aggregate in a fashion similar to the core-peptide, in spite of their R_9 tag. We fit the kinetic data of these aggregating peptides to growth curves, and results are summarized in Table I. None of the peptides had a significant lag time. The core-peptide showed the fastest aggregation, followed closely by the T-peptide ($k = 10.6\ sec^{-1}$ and $8.5\ sec^{-1}$, respectively). V-peptide and F-peptide aggregated with about a three times slower rate ($3.2–3.3\ sec^{-1}$), whereas VV-peptide

TABLE I. Summary of Data for the Peptides Studied

Peptide	Sequence[a]	Expected MW	Observed MW	Fitted kinetic parameters[b]		
				A	k (sec^{-1}) × 10^3	k′ (sec^{-1}) × 10^5
Core-peptide	Ac-vqivyk-NH_2	790	792	6.3	10.6	
T-peptide	Ac-vqivyk-R_9-NH_2	2,195	2,195	9.1	8.5	4.4
T(L)-peptide	Ac-VQIVYK-R_9-NH_2	2,195	2,195	—	—	—
V-peptide	Ac-vqvvyk-R_9-NH_2	2,182	2,184	10	3.2	4.8
VV-peptide	Ac-vqvvvk-R_9-NH_2	2,118	2,119	NA		
F-peptide	Ac-VQIVFK-R_9-NH_2	2,179	2,179	5.5	3.3	
K-peptide	Ac-vqivkk-R_9-NH_2	2,161	2,160	NA		
T-FITC-peptide	FITC-$(Ahx)_2$-vqivyk-R_9-NH_2	2,737	2,736	—	—	—

[a]Lower case amino acid codes denote D-amino acids.
[b]Fitting of kinetic data is described in the text (Eq. 1). NA indicates no aggregation was observed as monitored using ThS fluorescence. The absence of data indicates that no kinetics were measured. We estimate a ±10% error in fitted kinetic parameters.

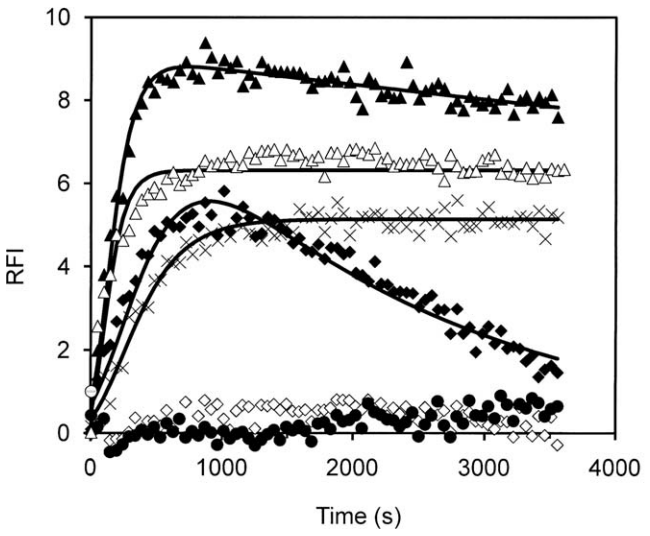

Fig. 1. Aggregation kinetics of peptides studied in vitro. Aggregation kinetics of T-peptide (solid triangles), V-peptide (solid lozenges), F-peptide (X), core-peptide (open triangles), VV-peptide (open lozenges), and K-peptide (circles). The figure shows the time dependence of the fluorescence intensity for 10 μM peptide, 33 μM heparin, and 100 μM ThS in buffer A. Solid lines represent fitted values.

and K-peptide showed no aggregation at the 10 μM concentration. In the case of the K-peptide, this finding is consistent with our previous observations showing that a lysine placed at position 5 in the core sequence results in a nonaggregating peptide (Rojas Quijano et al., 2006).

We characterized the morphology of the samples using TEM (Fig. 2). As we have shown to be the case previously, the core-peptide formed straight filaments, where each filament is formed from two axially aligned fibrils (7 ± 1 nm diameter; Rojas Quijano et al., 2006). Small amyloid bodies (20–40 nm in diameter) and irregular, nonuniform filaments were seen in the TEMs of the V-peptide and the F-peptide (not shown), whereas aggregated T-peptide contained left-handed twisted filaments with a diameter of 27 ± 4 nm and a half-periodicity of 134 ± 12 nm (n = 7). Among the peptides not showing significant ThS enhancement over time, irregularly shaped nonfibular aggregates appeared in the TEM of K-peptide, whereas flake-like, large spherical aggregates (430 ± 60 nm diameter) appeared in the VV-peptide preparation (not shown). We have previously observed such large spherical bodies for other peptides (Goux et al., 2004).

T-Peptide Is Highly Neurotoxic

We used cultured cerebellar granule neurons to test the effect of T-peptide exposure on neuronal survival. As shown in Figures 3 and 4, T-peptide induces cell death in a concentration-dependent manner, with significant death observable at doses of ≥5 μM. About 80% of the neurons were dead when treated with 10 μM of T-peptide. Cell viability results obtained using the Live/Dead assay were confirmed using the MTT assay, which reflects mitochondrial function (Fig. 3B). To rule out the possibility that the R_9 stretch was contributing to the neurotoxic action of T-peptide, we exposed cells to Ac-R_9-NH_2, a peptide composed of just the nine R residues. This peptide had no effect on neuronal survival (data not shown). To confirm that the toxic effect of T-peptide was due to its aggregation ability rather than chirality, we synthesized an L-version of the peptide in which the core as well as the R_9 tag was synthesized using L-amino acids. This peptide, T(L)-peptide, displayed a level of neurotoxicity that was similar to that of T-peptide (Figs. 3, 4).

T-peptide-treated neurons displayed disintegration of neurites and cell body shrinkage and fragmentation, suggesting that death was due to apoptosis. A characteristic feature of apoptotic death is nuclear condensation and fragmentation. To confirm that apoptosis was the mode by which T-peptide-mediated neuronal death occurs, we visualized nuclei using DAPI. Surprisingly, nuclei of neuronal cultures treated with T-peptide were rarely fragmented and were only slightly condensed (Fig. 5A). In contrast, neurons treated with nondepolarizing medium (low-potassium treatment), a stimulus known to induce apoptosis in cultured cerebellar granule neurons,

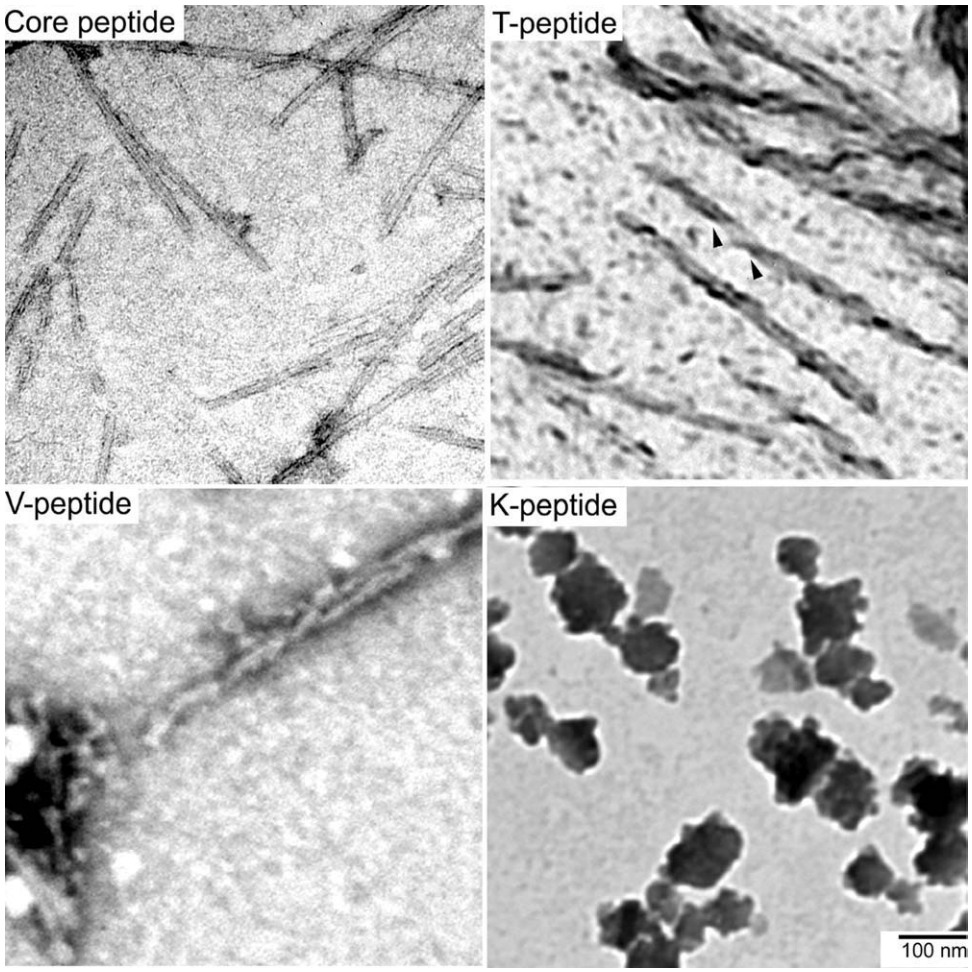

Fig. 2. TEM of peptides studied. TEM of core-peptide, T-peptide (arrows denote helical twist), V-peptide, and K-peptide. All peptides were prepared at 100 μM in buffer A and stained with uranyl acetate.

show robust nuclear condensation and fragmentation (Fig. 5A). Nuclei of T-peptide-treated neurons were also abnormally shaped and displayed a highly punctate staining pattern with DAPI (Fig. 5A). These results suggest that death induced by T-peptide occurred through a mechanism that was not fully apoptotic.

Another common mode of cell death, and one that occurs in a variety of in vitro and in vivo models of neurodegeneration, is autophagy. Autophagic death is characterized by the appearance of large numbers of vesicles called autophagosomes that are detectable by light microscopy. A reliable biochemical marker of autophagic cell death is the conversion of microtubule-associated protein light chain 3 (LC3) from a cytoplasmic form, referred to as LC-1, to a processed form, LC3-II, which is a component of the autophagosome membrane (Kabeya et al., 2000). Increase in LC3-II levels has been shown to correlate with autophagosome formation. We could not detect the formation of LC3-containing vesicles in T-peptide-treated neurons by immunocytochemistry (data not shown). Moreover, LC3-I cleavage to LC3-II was not increased in neurons that were degenerating after treatment with T-peptide (Fig. 5B). These observations suggest that death of neurons resulting from T-peptide exposure is not due to autophagy.

As observed with cerebellar granule neurons, T-peptide induces the death of cultured cortical neurons. However, cortical neurons were slightly less sensitive to T-peptide induced toxicity than cerebellar granule neurons (Fig. 6A). As observed with cerebellar granule neurons, no nuclear fragmentation was observed in T-peptide treated cortical neurons (data not shown).

T-Peptide Neurotoxicity Is Aggregation-Dependent and Is Enhanced by Cell Permeability

To examine whether aggregation is necessary for T-peptide-induced neurotoxicity, we synthesized three mutant peptides referred to as K-peptide, V-peptide, and VV-peptide (Table I). TEM and kinetic analyses reveal that neither K-peptide nor VV-peptide aggregate in vitro at concentrations used to measure toxicity. In contrast, V-peptide does form aggregates, albeit less efficiently than T-peptide. Although treatment of cerebellar granule

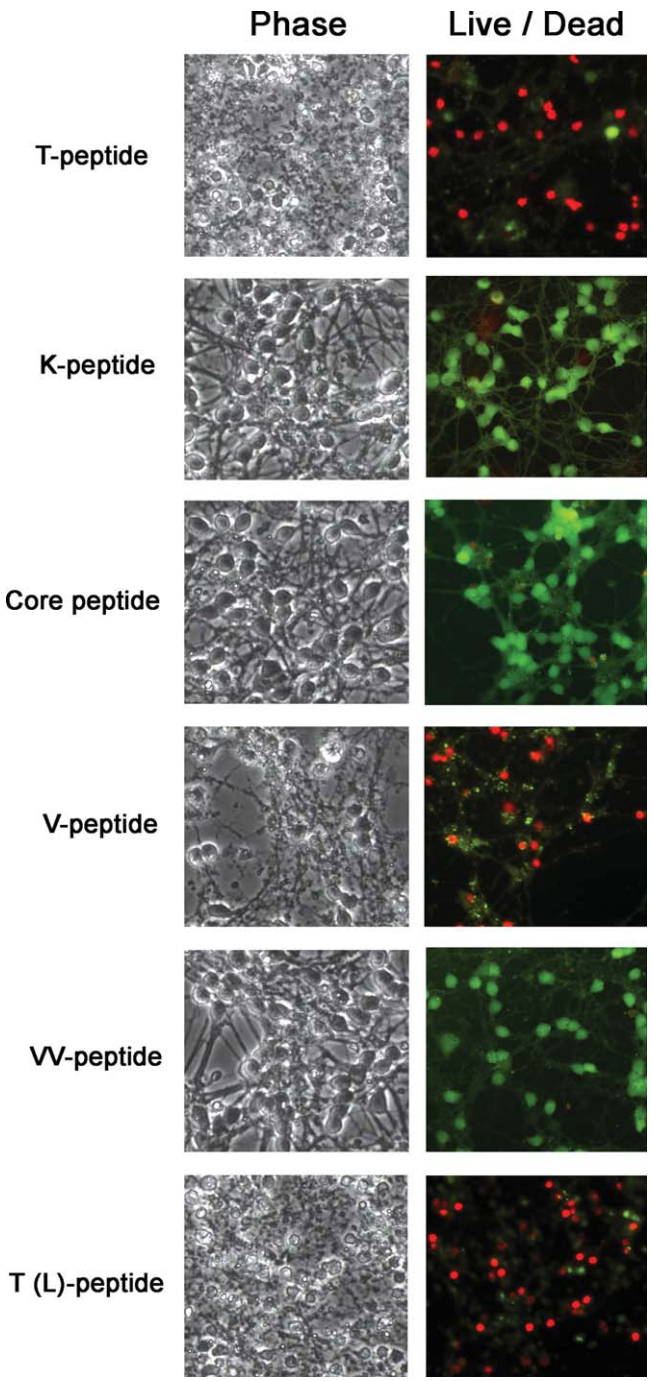

Fig. 3. Effects of tau peptides on survival of cerebellar granule neurons. Neuronal cultures were switched to serum-free medium containing T-peptide, K-peptide, core-peptide, V-peptide, VV-peptide, and T(L)-peptide. All peptides were used at 25 μM concentration. Phase-contrast micrographs show the appearance of the cultures after 24 hr of peptide treatment. The Live/Dead viability assay was also performed. Nuclei of dead cells are stained red, whereas the cytoplasm of living cells is stained green. In the case of sick and dying cells, green staining is condensed.

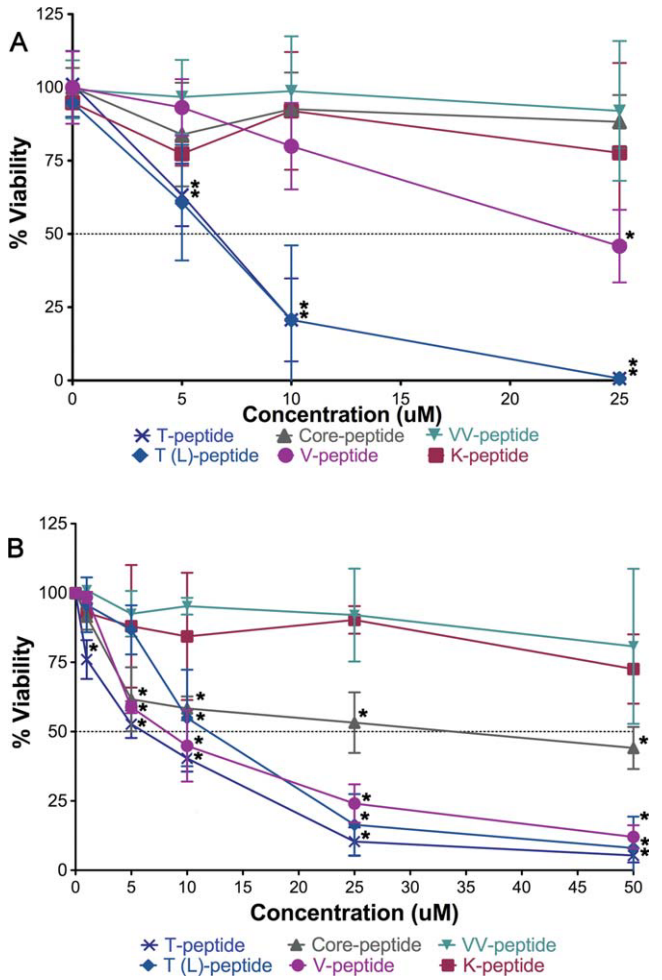

Fig. 4. Neuronal cell viability following treatment with tau peptides. Cerebellar granule neurons were switched to serum-free medium containing various concentrations of T-peptide, K-peptide, core-peptide, V-peptide, VV-peptide, and T(L)-peptide. Cell viability was measured using two independent methods 24 hr after peptide treatment, and results are graphed. *$P < 0.05$ compared with control cells that were treated with HK. **A**: Results from Live/Dead viability assay. **B**: Results from MTT assay.

neurons with V-peptide resulted in a moderate level of cell death (~50% cell death at 25 μM peptide concentration), neither K-peptide nor VV-peptide reduced neuronal survival, indicating that neurotoxicity is dependent on peptide aggregation (Figs. 3, 4).

Previous studies have shown that tau protein is toxic to neurons even when added extracellularly (Gomez-Ramos et al., 2006, 2008; Frost et al., 2009). To examine whether entry into the cell was required for T-peptide neurotoxicity, we treated cerebellar granule neurons with core-peptide. Phase-contrast microscopy and Live/Dead assays showed that core-peptide was not toxic (Figs. 3, 4A). This suggests that the neurotoxic effect of the hexameric tau sequence is mediated intracellularly. Surprisingly, given the healthy appearance of

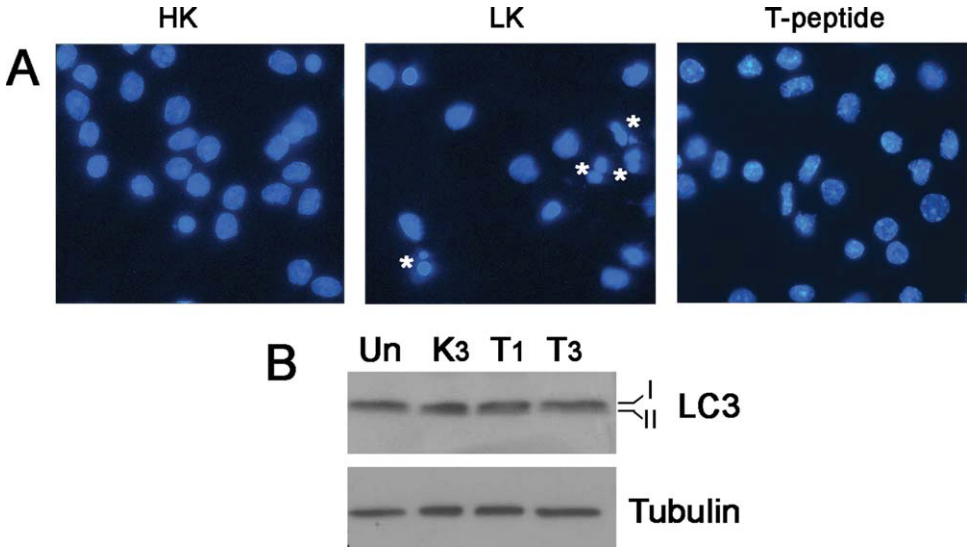

Fig. 5. Neurotoxicity by T-peptide occurs through a mechanism that is neither fully apoptotic nor autophagic. **A**: Nuclear morphology of cerebellar granule neurons treated with T-peptide. Cerebellar granule neuron cultures were treated with T-peptide in medium containing depolarizing levels of potassium (HK). The cultures were then fixed and stained with DAPI to visualize nuclear morphology. Sister cultures were treated for 24 hr with HK alone (in which they survive) or with nondepolarizing medium (5 mM KCl or LK) in which they undergo apoptosis. In contrast to the nuclear condensation and fragmentation (marked with asterisks) in LK-treated cultures, nuclei of cultures treated with T-peptide displayed no fragmentation. Large bright spots are visible in the nuclei of T-peptide-treated neurons. **B**: LC3 cleavage pattern following T-peptide treatment of neurons. Cerebellar granule neurons were either untreated (Un) or treated with K-peptide for 3 hr (K3) or with T-peptide for 1 and 3 hr (T1 and T3, respectively). Total cell lysates were prepared and subjected to Western blotting using an LC3 antibody. Although the 18-kDa cytoplasmic LC-I could be clearly detected, only a faint 16-kDa band representing the autophagosome-associated LC-II form of the LC3 protein could be detected. No alterations in the pattern of LC-I and LC-II were discernible. Lysates from cells treated with K- and T-peptide for 6 and 9 hr were also analyzed but yielded similar results (not shown). [Color figure can be viewed in the online issue, which is available at wileyonlinelibrary.com.]

the cultures and results from the Live/Dead assay, MTT assays revealed mitochondrial dysfunction in core-peptide-treated neurons (Fig. 4B).

Neurons Are Selectively Sensitive to T-Peptide Toxicity

In AD and other tauopathies, neurons are selectively affected. To examine whether T-peptide toxicity is similarly cell selective, we exposed primary cultures of kidney fibroblasts to it. Although these cells were also killed by T-peptide, they were much less sensitive than the two neuronal cell types (Fig. 6A). Primary glial cells are also less sensitive than neurons to T-peptide toxicity (data not shown).

We also treated two cell lines with T-peptide. Although the hippocampally derived HT-22 neuroblastoma cell line shows a moderate level of sensitivity, the human embryonic kidney HEK293T cell line is resistant at doses of up to 50 μM (Fig. 6B). These results indicate that neuronal cells are more vulnerable to the toxic effect of T-peptide than other cell types.

Peptide Aggregates Localize to the Nuclei Within Cells

To investigate whether T-peptide enters the cell, we synthesized and treated HT-22 cells with a fluorescent (FITC-conjugated) form of T-peptide. As shown in Figure 7, T-FITC enters the cell. Interestingly, the peptide localizes predominantly in the nucleus, appearing in large and distinct structures resembling aggregates.

To confirm that T-peptide forms aggregates, we used ThS, a dye that binds protein fibrils and aggregates. As observed with T-FITC, ThS staining also revealed distinct aggregate-like structures in the nucleus (Fig. 8). In addition to the nucleus, however, a significant level of staining was observed in the cytoplasm. Staining in the cytoplasm was diffuse compared with the punctate pattern in the nucleus. Positive staining with ThS in the nucleus and cytoplasm was also observed with V-peptide. In contrast, cultures treated with K-peptide were not stained with ThS.

Phosphorylation of T-Peptide Is Not Required for Aggregation or Neurotoxicity

Several studies have suggested that hyperphosphorylation of tau within the repeat regions causes its disassociation from microtubules and its assembly into fibrils (for review see Takashima, 2008). Moreover, selective and broad-range kinase inhibitors can reduce abnormal tau phosphorylation and aggregation in transgenic mice, affording protection against neuronal degeneration (Noble et al., 2005; Le Corre et al., 2006). Recent reports have established that tau is phosphorylated not only on serine and threonine but also on tyrosine

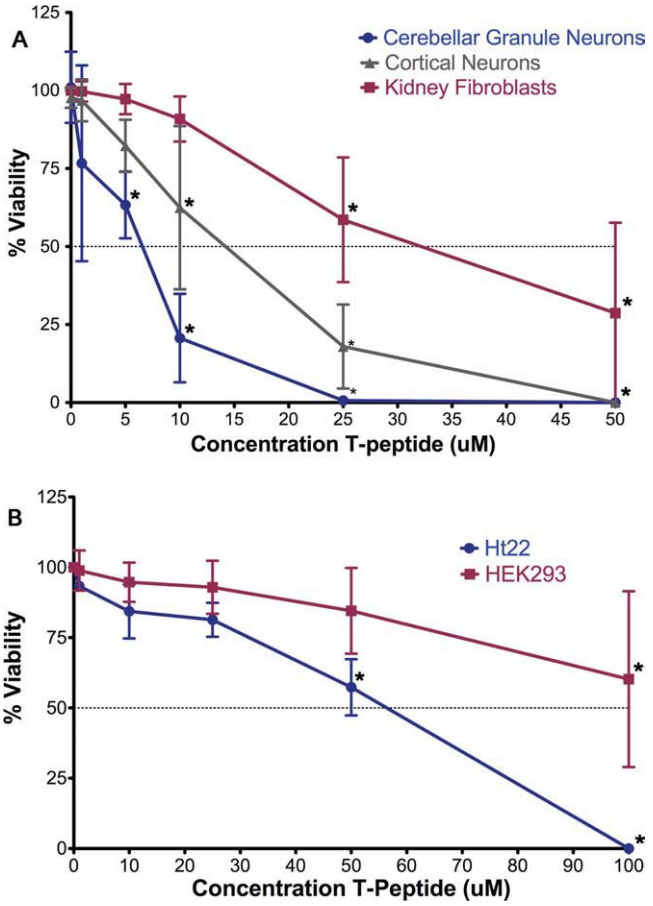

Fig. 6. Neuronal cells are selectively vulnerable to T-peptide toxicity. Primary cultures and cell lines were treated in serum-free medium with T-peptide for 24 hr. Viability was quantified using the Live/Dead assay. $*P < 0.05$ compared with control cells that were treated with serum-free medium without peptide. **A**: Results from the analyses of cerebellar granule neurons (in HK medium), cortical neurons, and kidney fibroblasts cultured from rats. **B**: Results from the HT22 and HEK293 cell lines.

residues (for review see Lebouvier et al., 2009). The hexameric sequence within T-peptide has a tyrosine residue, which is missing in the two nontoxic peptides, K-peptide and VV-peptide, but is present in the neurotoxic V-peptide. It was conceivable, therefore, that phosphorylation of the tyrosine residue within T-peptide was necessary for aggregation and neurotoxicity. To investigate this issue, we synthesized a peptide designated as F-peptide that has a phenylalanine residue instead of tyrosine. As shown in Table I, F-peptide is capable of self-aggregation in vitro. Treatment of neurons with F-peptide also induces toxicity (Fig. 9). Although the level of toxicity was slightly lower than that displayed by T-peptide, this likely reflects the lower aggregation ability of F-peptide compared with T-peptide. This result demonstrates that phosphorylation of T-peptide is not necessary for neurotoxicity and strengthens the conclusion that aggregation is the key requirement for neurotoxicity.

Fig. 7. Subcellular localization of T-peptide. HT-22 cells were treated with an FITC-tagged form of T-peptide (T-FITC-peptide) for 3 hr. Subcellular localization was visualized by fluorescence microscopy. The cells were also counterstained with DAPI (for nuclear morphology) and propidium iodide (PI; for cell viability). Note the intense and punctate staining in the nucleus. In comparison, cytoplasmic staining is generally diffuse.

Elevated Level on Tau Does Not Predispose Neurons to T-Peptide-Induced Death

The finding that neurons are selectively sensitive to T-peptide-induced toxicity raises the interesting possibility that the intracellular molecular composition of neurons is responsible for their higher sensitivity. One molecule expressed selectively in neurons that could confer such vulnerability is tau itself. In support of such a possibility is the finding that tau-deficient primary neurons are resistant to Aβ-induced toxicity (Rapoport et al., 2002; Liu et al., 2004). Furthermore, ectopic expression of tau fragments in cultured cells and transgenic mice has been reported in some studies, to promote aggregation of endogenous tau (Eckermann et al., 2007; Wang et al., 2007; Mocanu et al., 2008a). To examine the contribution of tau to T-peptide-induced neurotoxicity, we overexpressed human tau (2N-4R isoform) in neurons and then treated the cultures with T- or K-peptide. Overexpression of tau had no effect on cell viability by itself. Furthermore, the higher expression did not increase the extent of cell death that resulted from treatment with T-peptide (Fig. 10A,B).

Because T-peptide induces aggregation of cellular proteins and given the proposition that tau fragments including those containing the VQIVYK sequence have been shown to induce tau aggregation both in vivo and in cultured cells (Wang et al., 2007; Mocanu et al., 2008b; Frost et al., 2009), we investigated whether T-peptide causes aggregation of intracellular tau in neurons. As shown in Figure 10C,D, the overall pattern of ectopically expressed tau-YFP immunoreactivity was similar in neurons treated with T-peptide or K-peptide. Although the level of tau immunoreactivity was lower in T-peptide treated neurons, a similar finding was made in immunocytochemical analysis of endogenous tau protein (using a tau antibody) in untransfected neurons treated with the two peptides. The lack of a pattern of aggregation with either tau-YFP or endogeneous tau suggests that the aggregates stained with ThS in T-peptide-treated neurons are not composed of tau.

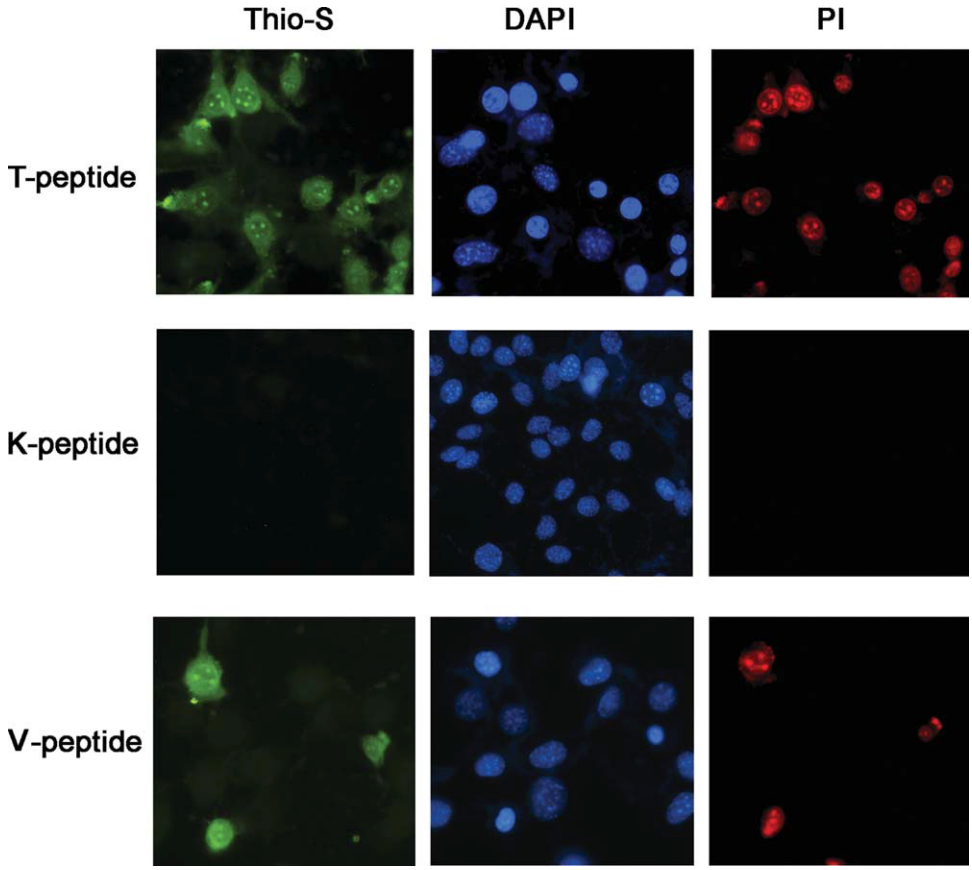

Fig. 8. T-peptide forms aggregates within the nuclei. Thioflavin-staining of T-peptide-treated cells. HT-22 cells were treated with T-peptide, K-peptide, and V-peptide. Three hours later, the cultures were stained with ThS (for aggregates), DAPI (for nuclear morphology), and propidium iodide (PI; for cell viability). Although staining is easily detectable in T-peptide- and V-peptide-treated cultures, it is not detectable in cultures treated with K-peptide. [Color figure can be viewed in the online issue, which is available at wileyonlinelibrary.com.]

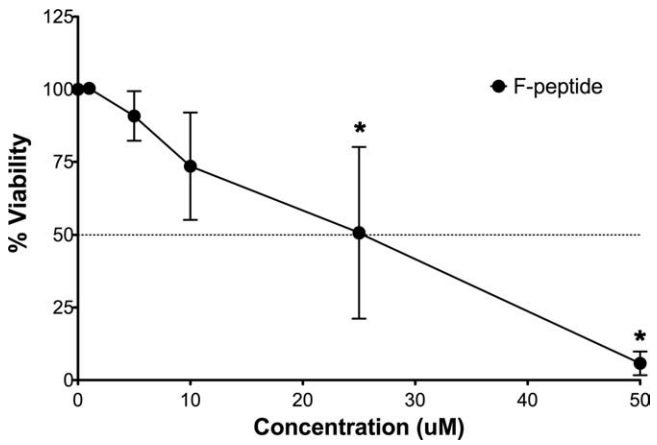

Fig. 9. Phosphorylation of T-peptide is not required for neurotoxicity. Cerebellar granule neurons were treated with different concentrations of F-peptide for 24 hr, after which cell viability was quantified using the red/green viability assay. F-peptide was synthesized using L-amino acids. $^*P < 0.05$ compared with control cells that were treated with HK.

Treatment With T-Peptide Results in the Down-Regulation of Endogenous Tau Levels

Although their role in promoting neuronal death remains to be resolved, hyperphosphorylation and aggregation of tau are known to occur in AD and other tauopathies (for review see Castellani et al., 2008). We examined whether tau was affected in neurons treated with T-peptide. As shown in Figure 11 and consistent with the reduced signal in immunocytochemical analysis, a reduction in the level of endogenous tau expression was discernible at 3 hr of T-peptide and was substantial by 6 hr. Tubulin expression was not altered. We have also examined the expression of other proteins in separate experiments and have found no change in response to treatment with T-peptide. To examine whether phosphorylation of tau was also affected, we used antibodies specific for tau phosphorylated at Ser404 and Ser262. As shown in Figure 11, the phosphorylation at both of these residues was also reduced. However, the reduction in phosphorylation between T-treated and core- or K-treated cultures

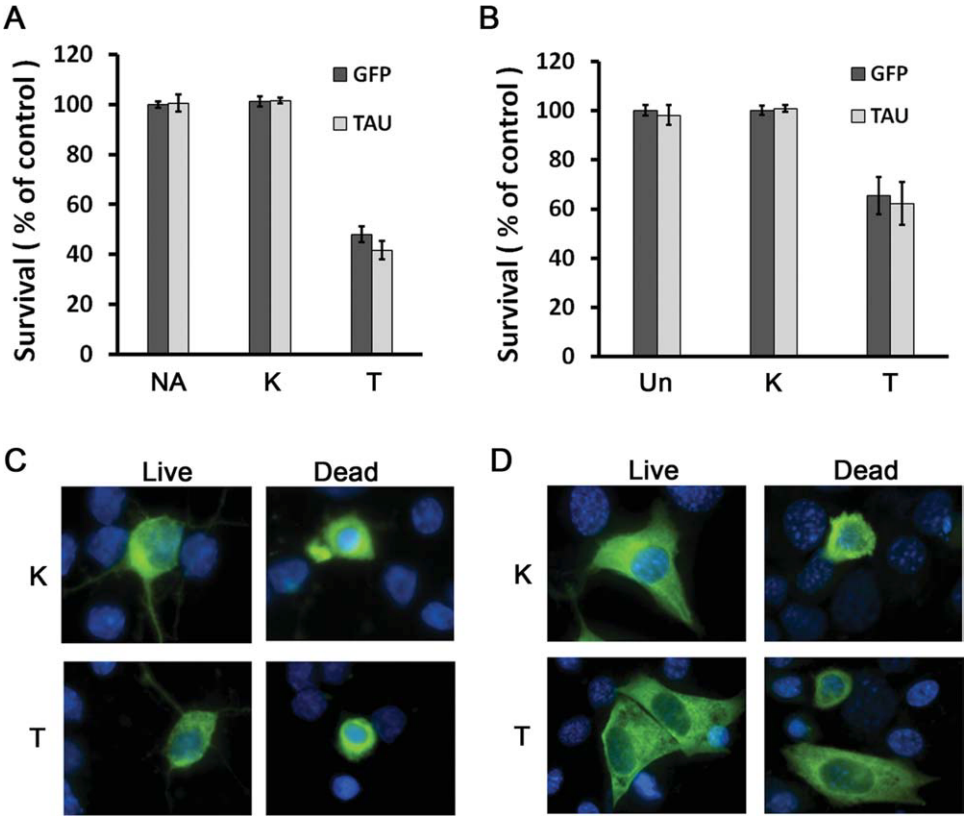

Fig. 10. Elevated level of intracellular tau does not increase neuronal vulnerability to T-peptide. Cerebellar granule neurons or HT-22 cells were transfected with expression plasmids encoding GFP or human tau-YFP. Proportion of transfected cells that were viable was quantified by DAPI staining. Pattern of tau-YFP localization was also evaluated after treatment with K- or T-peptide. Although few cells died following K-peptide treatment, representative images of tau localization in this small proportion of cells has been provided. **A**: Viability in cerebellar granule neurons. Transfected neuronal cultures were switched to HK medium containing no additives (NA), 10 μM K-peptide, or 10 μM T-peptide. Cell viability was quantified 24 hr later and normalized to viability of GFP-transfected neurons in HK. **B**: Viability in HT-22 cells. Cultures were either untreated (Un) or treated with 25 μM K-peptide or 25 μM T-peptide. Cell viability was quantified 24 hr later and normalized to viability of GFP-transfected untreated cultures. **C**: Localization of tau-YFP in healthy and dead neurons treated with K-peptide or T-peptide. **D**: Localization of tau-YFP in healthy and dead HT-22 cells treated with K-peptide or T-peptide. [Color figure can be viewed in the online issue, which is available at wileyonlinelibrary.com.]

was similar in extent to that observed with total tau antibody, suggesting that T-peptide does not have a significant effect on the phosphorylation of endogenous tau (Fig. 11).

T-Peptide Causes a Decrease in the Mitochondrial Membrane Potential

Although the MTT assay is commonly used to quantify cell viability, the assay actually evaluates mitochondrial function. Besides confirming loss of viability, our results using the MTT assay raises the possibility that T-peptide affects neuronal viability of cells via modulating the mitochondrial membrane potential. Alteration in mitochondrial membrane potential and mitochondrial dysfunction are hallmarks of neurodegenerative diseases. To examine directly the effects of T-peptide on the mitochondrial membrane potential, we used the fluorescent cationic dye JC-1 (Reers et al., 1991). As shown in Figure 12, our results indicate that T-peptide caused a reduction in the mitochondrial membrane potential of HT-22 cells in a concentration-dependent manner. Similarly, T(L)-peptide also resulted in a reduction in the mitochondrial membrane potential in a dose-dependent manner. In contrast, there was very little change in the mitochondrial membrane potential when K-peptide was added to HT-22 cells (Fig. 12). Core-peptide also caused a reduction in the mitochondrial membrane potential of HT-22 cells when added at high concentrations, in agreement with our results obtained in MTT assays (Fig. 12).

Other Aggregating Peptides Unrelated to Tau Are Not Neurotoxic

Although our data indicate that aggregation of T-peptide is required for neurotoxicity, thet do not rule out the possibility that any aggregating peptide, regardless of the sequences that compose it, would also be toxic. To examine this issue, we synthesized two peptides, STVIIE-R_9 (designated ST-peptide), previously described by Pastor et al. (2008), and another de novo

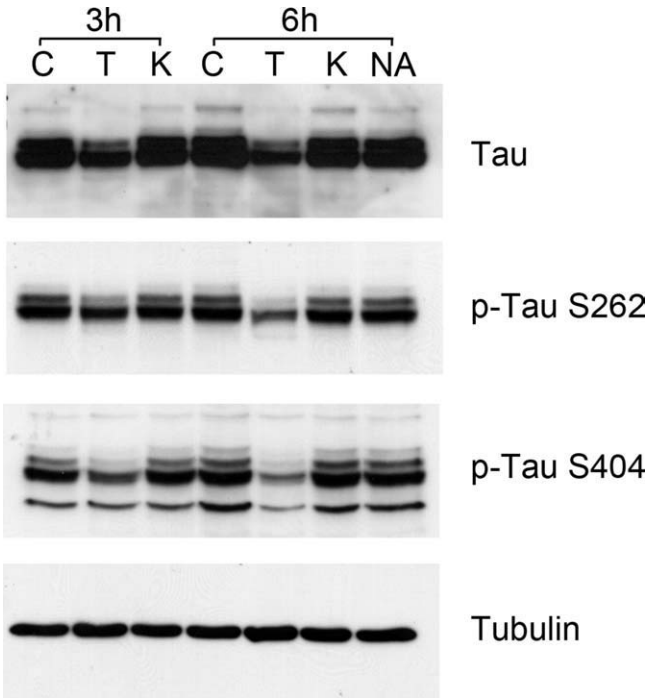

Fig. 11. Expression of endogenous tau is reduced by T-peptide. Cerebellar granule neurons were treated for 3 or 6 hr with HK medium containing no additives (NA) or 10 μM each of core-peptide (C), T-peptide (T), and K-peptide (K). Cell lysates were prepared and subjected to Western blot analysis using antibodies against total tau, Ser262-phospho-tau, and Ser404-phospho-tau. The blot was also probed with tubulin antibody to verify that similar amounts of protein were loaded in each lane.

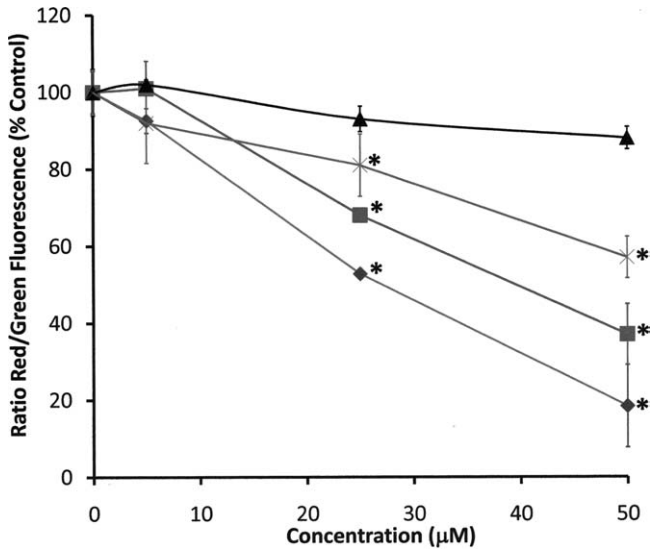

Fig. 12. Effects of tau peptides on the mitochondrial membrane potential of HT-22 cells. HT-22 cells were treated with various concentrations of T-peptide (lozenges), K-peptide (triangles), core-peptide (crosses), or T(L)-peptide (squares) for 24 hr in serum-free medium. The mitochondrial membrane potential of the cells was measured using the fluorescent dye JC-1. Cells were labeled with JC-1 solution for 2 hr at 37°C. Samples were imaged using a fluorescent plate reader set to detect both red and green fluorescence. The ratio of the red to green fluorescence units is a measure of the mitochondrial membrane potential. $*P < 0.05$ compared with nontreated control cells. [Color figure can be viewed in the online issue, which is available at wileyonlinelibrary.com.]

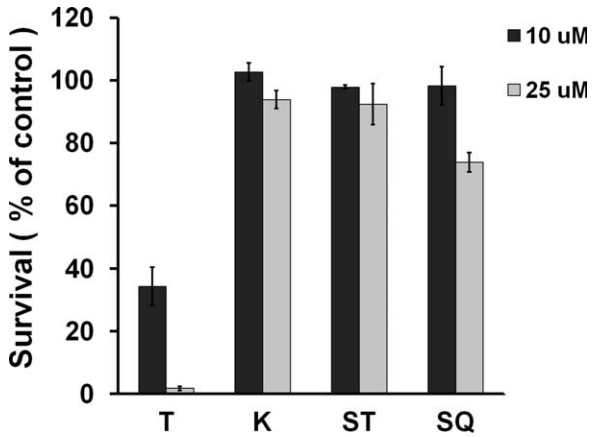

Fig. 13. Nontau-related aggregating peptides are not neurotoxic. Cerebellar granule neurons were treated in HK medium with T-, K-, ST-, and SQ-peptides at 10 and 25 μM concentrations. Viability was quantified 24 hr later and compared with K-peptide-treated cultures.

peptide, SQIVYA-R_9 (designated SQ-peptide). We were able to follow the kinetics of aggregation of both peptides into amyloid-forming structures using the fluorescence of ThS, and we characterized their morphology by TEM. The ST-peptide aggregated quite slowly over about a 3,000-sec lag time, after which it showed a second period of more rapid aggregation kinetics ($A = 4.9$, $k = 1.6 \times 10^{-3}$ sec^{-1}; $A' = 6.3$, $k' = 5.1 \times 10^{-3}$ sec^{-1} according to Eq. 2), whereas SQ-peptide showed kinetics similar to those of V-peptide ($A = 8.8$, $k = 3.8 \times 10^{-3}$ sec^{-1}). The ST-peptide formed amyloid sheets, which appeared to roll into irregular fibers 10–40 nm in diameter, whereas the SQ-peptide formed irregular, nonuniform filaments similar to those of V-peptide (Fig. 2). As shown in Figure 13, neither of these two peptides displayed neurotoxicity when tested in culture. This suggests that, in addition to its ability to aggregate, the neurotoxic action of T-peptide is dependent on its sequence.

DISCUSSION

We describe the establishment of a convenient cell culture model for studying the molecular mechanisms underlying tau neurotoxicity using an exogenously provided synthetic peptide containing the sequence VQIVYK located in the R3 region of tau. This hexameric sequence is known to self-assemble into fibrils robustly and with rapid kinetics. The presence of this hexameric motif within full-length tau and tau fragments is necessary for their oligomerization into a β-sheet conforma-

tion (Sahara et al., 2007). Moreover, this sequence is part of the protease-resistant PHF core identified in AD brains and of tau fragments found in AD and in experimental models of AD (Gamblin et al., 2003).

How does this model relate to the neurodegeneration observed in AD? In AD, aggregated tau deposits first appear in the entorhinal cortex, spreading to the hippocampus and eventually to most of the cortex. The gradual spreading of tau aggregates and neurodegeneration raises the possibility that healthy neurons and brain regions are exposed to some exogenous toxic factor released from degenerating neurons. It has been proposed that extracellular tau and proteolytic fragments of it could itself represent the toxic factor (Gomez-Ramos et al., 2006; Hernandez and Avila, 2008; Frost et al., 2009). Besides being released from dying neurons, tau fragments could leech out from tau ''ghost tangles''. It is likely that toxic tau fragments contain within them sequences such as the T-peptide core sequence, which are capable of initiating fibrillization of the fragment. Although we have facilitated cell entry by addition of the R_9 tag in our model system, it is possible that in disease states tau fragments are taken up by neurons, albeit inefficiently, by other mechanisms. Cytotoxicity by extracellularly located aggregating peptides has been described by other investigators, and mechanisms such as interaction of aggregated peptide with lipids of the membrane, formation of membrane pores, and alterations in membrane properties such as conductance or fluidity have been suggested (Kayed et al., 2004; Rochet et al., 2004; Quist et al., 2005; Singer and Dewji, 2006). In our study, core-peptide, which lacks the cell-permeabilizing R_9 tag, is not significantly neurotoxic. These analyses were done at 24 hr after peptide treatment. It is possible that long-term treatment with core-peptide would elicit some neurotoxicity, as others have reported with full-length or fragments of tau.

Whether tau aggregation is protective or harmful has been an unresolved issue. Our results indicate that aggregation of tau is necessary for neurotoxicity. Two separate mutant forms of the T-peptide that are incapable of assembling into filaments (K-peptide and VV-peptide) are not toxic, whereas two other mutant forms of the peptide that are capable of aggregating (V-peptide and F-peptide) are toxic. These results are consistent with previously published studies in which tau toxicity was found to be higher in cell lines transfected with an aggregation-prone mutant form of tau, whereas cells expressing aggregation-deficient mutants showed reduced toxicity (Khlistunova et al., 2006, 2007). Also consistent with an essential role for aggregation is the finding that pharmacological antagonists of aggregation are protective in mammalian cell culture and *Drosophila* models of tau neurotoxicity (Berger et al., 2006; Khlistunova et al., 2006, 2007). Interestingly, other hexameric peptides with sequences unrelated to T-peptide or tau but capable of aggregating efficiently in vitro do not display neurotoxicity. This suggests that, although aggregation is necessary for neurotoxicity, degeneration induced by T-peptide is dependent on its sequence.

The effect of T-peptide on cell viability was studied on several different types of primary cells and cell lines. These included cultures of cerebellar granule neurons, cortical neurons, cortical glial cultures, and kidney fibroblasts, as well as HT-22 neuroblastoma and the embryonic kidney HEK293T cell lines. We find that primary neurons are most sensitive to T-peptide induced neurotoxicity. HT-22 cells were also moderately sensitive to T-peptide and showed a higher level of toxicity than either kidney fibroblasts or HEK293T cells. Although relative uptake of peptide and its stability have not been analyzed in the different cell types, this finding raises the interesting possibility that the intracellular molecular composition of neurons is responsible for their higher sensitivity to the toxic effects of aggregated T-peptide. Another effect of T-peptide-induced neurotoxicity that recapitulates AD and other neurodegenerative diseases is that it induces mitochondrial dysfunction as indicated by reduced membrane potential and lowered ability to reduce MTT to formazan.

The utilization of a fluorescently labeled form of T-peptide has permitted the determination of its subcellular localization. Although some staining is visible in the cytoplasm, T-peptide localizes predominantly to the nucleus. Interestingly, within the nucleus, T-peptide is in large aggregates. It is not clear whether the nuclear aggregates are composed solely of T-peptide or whether other proteins are also contained within them. ThS staining confirmed the presence of nuclear aggregates, but more staining with this dye was observed in the cytoplasm, where staining with fluorescent T-peptide is weak at best. These results suggest that the cytoplasmic aggregates, the formation of which is induced by T-peptide, are composed primarily of endogenous proteins. One candidate endogenous protein that could be induced to aggregate in response to T-peptide is tau. Previous studies have suggested that the fragments containing the hexameric sequence within T-peptide are capable of nucleating fibrillization of full-length tau in cultured cells as well as transgenic mice (Wang et al., 2007; Mocanu et al., 2008b; Frost et al., 2009). To examine this possibility, we examined the effect of T-peptide on the localization of endogenous tau and transfected tau-YFP. Interestingly, T-peptide had no effect on the distribution or appearance of intracellular tau, arguing against the possibility that neurotoxicity of T-peptide was mediated through the aggregation of endogenous tau. Although not affecting localization, treatment with T-peptide does result in a dramatic reduction in tau levels. Fractionation of soluble and insoluble tau from T-peptide-treated neurons showed a distribution similar to that of neurons treated with K-peptide (data not shown), ruling out the possibility that the reduction is due to the conversion of tau into an insoluble form through aggregation. Another possibility is that T-peptide induces the proteolytic cleavage of tau. Such cleavage of tau is known to occur in AD and in other experimental models of neurodegeneration (Canu et al., 1998; Gamblin et al., 2003; Corsetti et al., 2008).

In summary, we have established a tissue culture model that recapitulates features of the selective degeneration of neurons seen in AD. Although it is unclear whether the hexameric peptide itself is present in AD brain or cerebrospinal fluid, it is within the 12-kDa tau protein protease-resistant minimal component of PHFs isolated from AD brains (Wischik et al., 1988a,b; Jakes et al., 1991; Novak et al., 1993). It is also part of tau fragments produced in AD brains and experimental models that are capable of promoting neurodegeneration when expressed in experimental systems (Gamblin et al., 2003). We propose that, once released by dying neurons, such tau fragments could be taken up by healthy neurons by an endocytotic mechanism and cause a reduction in endogenous tau levels, possibly through the induction of proteolytic cleavage. Mitochondrial dysfunction, another characteristic feature of AD, is also observed following exposure to T-peptide. The tissue culture model that we have described can be used to study the molecular mechanisms underlying tau neurotoxicity. Moreover, it is amenable to high-throughput screening of chemical libraries for blockers of tau fragment fibrillization or its cytotoxic effect on neurons and neuronal cell lines. Our results also suggest that an immunotherapeutic approach specifically targeting the hexameric sequence within T-peptide might reduce neurodegeneration in AD and other tauopathies.

ACKNOWLEDGMENT

The tau-YFP plasmid was kindly provided by Dr. Marc Diamond (Washington University School of Medicine).

REFERENCES

Allen MJ, MacRenaris KW, Venkatasubramanian PN, Meade TJ. 2004. Cellular delivery of MRI contrast agents. Chem Biol 11:301–307.

Alonso Adel C, Li B, Grundke-Iqbal I, Iqbal K. 2006. Polymerization of hyperphosphorylated tau into filaments eliminates its inhibitory activity. Proc Natl Acad Sci U S A 103:8864–8869.

Andorfer C, Acker CM, Kress Y, Hof PR, Duff K, Davies P. 2005. Cell-cycle reentry and cell death in transgenic mice expressing nonmutant human tau isoforms. J Neurosci 25:5446–5454.

Ballatore C, Lee VM, Trojanowski JQ. 2007. Tau-mediated neurodegeneration in Alzheimer's disease and related disorders. Nat Rev Neurosci 8:663–672.

Barghorn S, Mandelkow E. 2002. Toward a unified scheme for the aggregation of tau into Alzheimer paired helical filaments. Biochemistry 41:14885–14896.

Berger Z, Ravikumar B, Menzies FM, Oroz LG, Underwood BR, Pangalos MN, Schmitt I, Wullner U, Evert BO, O'Kane CJ, Rubinsztein DC. 2006. Rapamycin alleviates toxicity of different aggregate-prone proteins. Hum Mol Genet 15:433–442.

Berger Z, Roder H, Hanna A, Carlson A, Rangachari V, Yue M, Wszolek Z, Ashe K, Knight J, Dickson D, Andorfer C, Rosenberry TL, Lewis J, Hutton M, Janus C. 2007. Accumulation of pathological tau species and memory loss in a conditional model of tauopathy. J Neurosci 27:3650–3662.

Canu N, Dus L, Barbato C, Ciotti MT, Brancolini C, Rinaldi AM, Novak M, Cattaneo A, Bradbury A, Calissano P. 1998. Tau cleavage and dephosphorylation in cerebellar granule neurons undergoing apoptosis. J Neurosci 18:7061–7074.

Castellani RJ, Nunomura A, Lee HG, Perry G, Smith MA. 2008. Phosphorylated tau: toxic, protective, or none of the above. J Alzheimers Dis 14:377–383.

Chen HM, Wang L, D'Mello SR. 2008. Inhibition of ATF-3 expression by B-Raf mediates the neuroprotective action of GW5074. J Neurochem 105:1300–1312.

Corsetti V, Amadoro G, Gentile A, Capsoni S, Ciotti MT, Cencioni MT, Atlante A, Canu N, Rohn TT, Cattaneo A, Calissano P. 2008. Identification of a caspase-derived N-terminal tau fragment in cellular and animal Alzheimer's disease models. Mol Cell Neurosci 38:381–392.

Ding H, Johnson GV. 2008. The last tangle of tau. J Alzheimers Dis 14:441–447.

D'Mello SR, Galli C, Ciotti T, Calissano P. 1993. Induction of apoptosis in cerebellar granule neurons by low potassium: inhibition of death by insulin-like growth factor I and cAMP. Proc Natl Acad Sci U S A 90:10989–10993.

Eckermann K, Mocanu MM, Khlistunova I, Biernat J, Nissen A, Hofmann A, Schonig K, Bujard H, Haemisch A, Mandelkow E, Zhou L, Rune G, Mandelkow EM. 2007. The beta-propensity of Tau determines aggregation and synaptic loss in inducible mouse models of tauopathy. J Biol Chem 282:31755–31765.

Feany MB, Dickson DW. 1996. Neurodegenerative disorders with extensive tau pathology: a comparative study and review. Ann Neurol 40:139–148.

Frost B, Jacks RL, Diamond MI. 2009. Propagation of tau misfolding from the outside to the inside of a cell. J Biol Chem 284:12845–12852.

Futaki S. 2002. Arginine-rich peptides: potential for intracellular delivery of macromolecules and the mystery of the translocation mechanisms. Int J Pharmacol 245:1–7.

Futaki S, Suzuki T, Ohashi W, Yagami T, Tanaka S, Ueda K, Sugiura Y. 2001. Arginine-rich peptides. An abundant source of membrane-permeable peptides having potential as carriers for intracellular protein delivery. J Biol Chem 276:5836–5840.

Gamblin TC, Chen F, Zambrano A, Abraha A, Lagalwar S, Guillozet AL, Lu M, Fu Y, Garcia-Sierra F, LaPointe N, Miller R, Berry RW, Binder LI, Cryns VL. 2003. Caspase cleavage of tau: linking amyloid and neurofibrillary tangles in Alzheimer's disease. Proc Natl Acad Sci U S A 100:10032–10037.

Gomez-Ramos A, Diaz-Hernandez M, Cuadros R, Hernandez F, Avila J. 2006. Extracellular tau is toxic to neuronal cells. FEBS Lett 580:4842–4850.

Gomez-Ramos A, Diaz-Hernandez M, Rubio A, Miras-Portugal MT, Avila J. 2008. Extracellular tau promotes intracellular calcium increase through M1 and M3 muscarinic receptors in neuronal cells. Mol Cell Neurosci 37:673–681.

Goux WJ, Kopplin L, Nguyen AD, Leak K, Rutkofsky M, Shanmuganandam VD, Sharma D, Inouye H, Kirschner DA. 2004. The formation of straight and twisted filaments from short tau peptides. J Biol Chem 279:26868–26875.

Hernandez F, Avila J. 2008. Tau aggregates and tau pathology. J Alzheimers Dis 14:449–452.

Honson NS, Kuret J. 2008. Tau aggregation and toxicity in tauopathic neurodegenerative diseases. J Alzheimers Dis 14:417–422.

Jakes R, Novak M, Davison M, Wischik CM. 1991. Identification of 3- and 4-repeat tau isoforms within the PHF in Alzheimer's disease. EMBO J 10:2725–2729.

Kabeya Y, Mizushima N, Ueno T, Yamamoto A, Kirisako T, Noda T, Kominami E, Ohsumi Y, Yoshimori T. 2000. LC3, a mammalian homologue of yeast Apg8p, is localized in autophagosome membranes after processing. EMBO J 19:5720–5728.

Kayed R, Sokolov Y, Edmonds B, McIntire TM, Milton SC, Hall JE, Glabe CG. 2004. Permeabilization of lipid bilayers is a common conformation-dependent activity of soluble amyloid oligomers in protein misfolding diseases. J Biol Chem 279:46363–46366.

Khlistunova I, Biernat J, Wang Y, Pickhardt M, von Bergen M, Gazova Z, Mandelkow E, Mandelkow EM. 2006. Inducible expression of Tau repeat domain in cell models of tauopathy: aggregation is toxic to cells but can be reversed by inhibitor drugs. J Biol Chem 281:1205–1214.

Khlistunova I, Pickhardt M, Biernat J, Wang Y, Mandelkow EM, Mandelkow E. 2007. Inhibition of tau aggregation in cell models of tauopathy. Curr Alzheimer Res 4:544–546.

Koulich E, Nguyen T, Johnson K, Giardina C, D'mello S. 2001. NF-kappaB is involved in the survival of cerebellar granule neurons: association of IkappaBbeta [correction of Ikappabeta] phosphorylation with cell survival. J Neurochem 76:1188–1198.

Le Corre S, Klafki HW, Plesnila N, Hubinger G, Obermeier A, Sahagun H, Monse B, Seneci P, Lewis J, Eriksen J, Zehr C, Yue M, McGowan E, Dickson DW, Hutton M, Roder HM. 2006. An inhibitor of tau hyperphosphorylation prevents severe motor impairments in tau transgenic mice. Proc Natl Acad Sci U S A 103:9673–9678.

Lebouvier T, Scales TM, Williamson R, Noble W, Duyckaerts C, Hanger DP, Reynolds CH, Anderton BH, Derkinderen P. 2009. The microtubule-associated protein tau is also phosphorylated on tyrosine. J Alzheimers Dis (in press).

Liu T, Perry G, Chan HW, Verdile G, Martins RN, Smith MA, Atwood CS. 2004. Amyloid-beta-induced toxicity of primary neurons is dependent upon differentiation-associated increases in tau and cyclin-dependent kinase 5 expression. J Neurochem 88:554–563.

Majdzadeh N, Wang L, Morrison BE, Bassel-Duby R, Olson EN, D'Mello SR. 2008. HDAC4 inhibits cell-cycle progression and protects neurons from cell death. Dev Neurobiol 68:1076–1092.

Mocanu MM, Nissen A, Eckermann K, Khlistunova I, Biernat J, Drexler D, Petrova O, Schonig K, Bujard H, Mandelkow E, Zhou L, Rune G, Mandelkow EM. 2008a. The potential for beta-structure in the repeat domain of tau protein determines aggregation, synaptic decay, neuronal loss, and coassembly with endogenous Tau in inducible mouse models of tauopathy. J Neurosci 28:737–748.

Mocanu MM, Nissen A, Eckermann K, Khlistunova I, Biernat J, Drexler D, Petrova O, Schonig K, Bujard H, Mandelkow E, Zhou L, Rune G, Mandelkow EM. 2008b. The potential for beta-structure in the repeat domain of tau protein determines aggregation, synaptic decay, neuronal loss, and coassembly with endogenous tau in inducible mouse models of tauopathy. J Neurosci 28:737–748.

Necula M, Kuret J. 2004. Pseudophosphorylation and glycation of tau protein enhance but do not trigger fibrillization in vitro. J Biol Chem 279:49694–49703.

Noble W, Planel E, Zehr C, Olm V, Meyerson J, Suleman F, Gaynor K, Wang L, LaFrancois J, Feinstein B, Burns M, Krishnamurthy P, Wen Y, Bhat R, Lewis J, Dickson D, Duff K. 2005. Inhibition of glycogen synthase kinase-3 by lithium correlates with reduced tauopathy and degeneration in vivo. Proc Natl Acad Sci U S A 102:6990–6995.

Novak M, Kabat J, Wischik CM. 1993. Molecular characterization of the minimal protease resistant tau unit of the Alzheimer's disease paired helical filament. EMBO J 12:365–370.

Pastor MT, Kummerer N, Schubert V, Esteras-Chopo A, Dotti CG, Lopez de la Paz M, Serrano L. 2008. Amyloid toxicity is independent of polypeptide sequence, length and chirality. J Mol Biol 375:695–707.

Quist A, Doudevski I, Lin H, Azimova R, Ng D, Frangione B, Kagan B, Ghiso J, Lal R. 2005. Amyloid ion channels: a common structural link for protein-misfolding disease. Proc Natl Acad Sci U S A 102:10427–10432.

Rapoport M, Dawson HN, Binder LI, Vitek MP, Ferreira A. 2002. Tau is essential to beta-amyloid-induced neurotoxicity. Proc Natl Acad Sci U S A 99:6364–6369.

Reers M, Smith TW, Chen LB. 1991. J-aggregate formation of a carbocyanine as a quantitative fluorescent indicator of membrane potential. Biochemistry 30:4480–4486.

Rochet JC, Outeiro TF, Conway KA, Ding TT, Volles MJ, Lashuel HA, Bieganski RM, Lindquist SL, Lansbury PT. 2004. Interactions among alpha-synuclein, dopamine, and biomembranes: some clues for understanding neurodegeneration in Parkinson's disease. J Mol Neurosci 23:23–34.

Rojas Quijano FA, Morrow D, Wise BM, Brancia FL, Goux WJ. 2006. Prediction of nucleating sequences from amyloidogenic propensities of tau-related peptides. Biochemistry 45:4638–4652.

Sahara N, Maeda S, Murayama M, Suzuki T, Dohmae N, Yen SH, Takashima A. 2007. Assembly of two distinct dimers and higher-order oligomers from full-length tau. Eur J Neurosci 25:3020–3029.

Santacruz K, Lewis J, Spires T, Paulson J, Kotilinek L, Ingelsson M, Guimaraes A, DeTure M, Ramsden M, McGowan E, Forster C, Yue M, Orne J, Janus C, Mariash A, Kuskowski M, Hyman B, Hutton M, Ashe KH. 2005. Tau suppression in a neurodegenerative mouse model improves memory function. Science 309:476–481.

Schneider A, Biernat J, von Bergen M, Mandelkow E, Mandelkow EM. 1999. Phosphorylation that detaches tau protein from microtubules (Ser262, Ser214) also protects it against aggregation into Alzheimer paired helical filaments. Biochemistry 38:3549–3558.

Singer SJ, Dewji NN. 2006. Evidence that Perutz's double-beta-stranded subunit structure for beta-amyloids also applies to their channel-forming structures in membranes. Proc Natl Acad Sci U S A 103:1546–1550.

Sun A, Nguyen XV, Bing G. 2002. Comparative analysis of an improved thioflavin-s stain, Gallyas silver stain, and immunohistochemistry for neurofibrillary tangle demonstration on the same sections. J Histochem Cytochem 50:463–472.

Suzuki T, Futaki S, Niwa M, Tanaka S, Ueda K, Sugiura Y. 2002. Possible existence of common internalization mechanisms among arginine-rich peptides. J Biol Chem 277:2437–2443.

Takashima A. 2008. Hyperphosphorylated tau is a cause of neuronal dysfunction in tauopathy. J Alzheimers Dis 14:371–375.

Vauthey S, Santoso S, Gong H, Watson N, Zhang S. 2002. Molecular self-assembly of surfactant-like peptides to form nanotubes and nanovesicles. Proc Natl Acad Sci U S A 99:5355–5360.

Ventura S, Zurdo J, Narayanan S, Parreno M, Mangues R, Reif B, Chiti F, Giannoni E, Dobson CM, Aviles FX, Serrano L. 2004. Short amino acid stretches can mediate amyloid formation in globular proteins: the Src homology 3 (SH3) case. Proc Natl Acad Sci U S A 101:7258–7263.

von Bergen M, Friedhoff P, Biernat J, Heberle J, Mandelkow EM, Mandelkow E. 2000. Assembly of tau protein into Alzheimer paired helical filaments depends on a local sequence motif (^{306}VQIVYK^{311}) forming beta structure. Proc Natl Acad Sci U S A 97:5129–5134.

von Bergen M, Barghorn S, Li L, Marx A, Biernat J, Mandelkow EM, Mandelkow E. 2001. Mutations of tau protein in frontotemporal dementia promote aggregation of paired helical filaments by enhancing local beta-structure. J Biol Chem 276:48165–48174.

von Bergen M, Barghorn S, Muller SA, Pickhardt M, Biernat J, Mandelkow EM, Davies P, Aebi U, Mandelkow E. 2006. The core of tau-paired helical filaments studied by scanning transmission electron microscopy and limited proteolysis. Biochemistry 45:6446–6457.

Wang YP, Biernat J, Pickhardt M, Mandelkow E, Mandelkow EM. 2007. Stepwise proteolysis liberates tau fragments that nucleate the Alzheimer-like aggregation of full-length tau in a neuronal cell model. Proc Natl Acad Sci U S A 104:10252–10257.

Wischik CM, Novak M, Edwards PC, Klug A, Tichelaar W, Crowther RA. 1988a. Structural characterization of the core of the paired helical filament of Alzheimer disease. Proc Natl Acad Sci U S A 85:4884–4888.

Wischik CM, Novak M, Thogersen HC, Edwards PC, Runswick MJ, Jakes R, Walker JE, Milstein C, Roth M, Klug A. 1988b. Isolation of a fragment of tau derived from the core of the paired helical filament of Alzheimer disease. Proc Natl Acad Sci U S A 85:4506–4510.